Pergamon

0021–9169(94)00133–2

Mesopause temperatures and integrated band brightnesses calculated from airglow OH emissions recorded at Maynooth (53.2°N, 6.4°W) during 1993

F. J. Mulligan, D. F. Horgan, J. G. Galligan and E. M. Griffin

Department of Experimental Physics, St. Patrick's College, Maynooth, Co. Kildare, Ireland

Abstract—Spectra of the hydroxyl emissions in the wavelength range 1.0–1.6 μm, which originate at mesopause altitudes, have been obtained, using a Fourier transform spectrometer at Maynooth (53.2°N, 6.4°W), on all suitable nights during the period January–December 1993. Rotational temperatures and integrated band brightnesses have been calculated from the spectra of the OH(3, 1) and (4, 2) vibration–rotation bands. The mean annual temperatures calculated over all measurements were $T(3, 1) = 200 \pm 19$ K and $T(4, 2) = 206 \pm 19$ K, where the uncertainty represents the standard deviation on the measurements. Harmonic analysis of the nightly averaged temperature values revealed an amplitude of 27 ± 1 K and a phase of 95 ± 2 days in the annual variation of the (3, 1) band at our latitude. The semiannual component was found to have an amplitude of 7 ± 1 K and a phase of -51 ± 9 days for this band. Results for the (4, 2) band were identical in both amplitude and phase for the annual component, while the semiannual component gave an amplitude of 8 ± 1 K and a phase of -43 ± 7 days. These results are compared with data recorded by the SME satellite, and with the predictions of the MSISE-90 model for a station at 53° latitude. Temperatures predicted by the MSISE-90 model for Maynooth are consistently below the values obtained in this study by 15–20 K. Excellent agreement is observed between the absolute value of temperature, in the case of the SME satellite, and in the amplitude and phase of the annual variation predicted by MSISE-90. The phase of the semiannual component observed in our data deviates somewhat from the -99 ± 1 days predicted by MSISE-90.

The annual mean brightness of the OH (3, 1) band was found to be 75 ± 18 kR, while that of the (4, 2) band was 106 ± 26 kR. Diurnal variations generally showed a steady decrease from dusk to dawn, apart from a brief period in June and July. Monthly average values of band brightness have been calculated for each band and are compared with the predictions of a recent photochemical model (Le Texier *et al.*, 1987). The model shows some elements of agreement with our observations, particularly a pair of maxima near the equinoxes, but it does not predict the broad winter maximum observed in both bands at this latitude.

1. INTRODUCTION

Hydroxyl airglow emissions emanating from the altitude region near the mesopause have been studied extensively since their original identification by Meinel in 1950 (Meinel, 1950a, 1950b). Sivjee (1992) has recently provided a comprehensive summary of experimental and theoretical work connected with these bands. The two parameters most frequently derived from ground based observations of these emissions are the integrated band brightness, and rotational temperature of the emitting region. The mean altitude profile of the hydroxyl band which shows a maximum at about 87 km, as discussed by Baker and Stair (1988), make it particularly suitable as a monitor of mesopause temperature. Sequences of observations are used to study temporal variations in rotational temperature and band brightness, and correlated

fluctuations of both parameters have been a subject of much investigation since Krassovsky (1972) first suggested acoustic-gravity waves as a source of these fluctuations. Quite a few measurements have been made at high latitude during polar winter (e.g. Hecht *et al*, 1987; Sivjee *et al*, 1987; Myrabo *et al.*, 1987; Viereck and Deehr, 1989; Hernandez *et al.*, 1992) on account of the opportunity of continuous observations, uninterrupted by daylight. Abreu and Yee (1989) have presented results from a study of diurnal and seasonal variations in the night-time OH (8-3) emission at low latitudes using data from the AE-E satellite. In spite of the extensive coverage that OH emissions have received in the literature over the past 40 years, many authors continue to stress the need for more observations of OH airglow. Theoretical models which predict the diurnal and seasonal variation of the brightness of these bands as a function of latitude

have been developed (Le Texier et al. 1987), but there are insufficient observations adequately to test these models (Abreu and Yee, 1989). Le Texier et al. (1987) have drawn attention to the potential of clarifying the transport of water vapour and odd oxygen near the mesopause through studies of OH emission as a function of vibrational level. The recent extension of the MSIS thermospheric model, into the middle and lower atmosphere, has highlighted differences between observations and the model near the mesopause (Hedin, 1991), demonstrating the need for additional measurements.

We report here values of rotational temperature and integrated band brightness calculated from a series of measurements of OH spectra made at Maynooth (53.2°N, 6.4°W) during 1993. Temperature results are compared with monthly averaged values derived from data recorded by the Solar Mesosphere Explorer (SME) satellite for the period 1982–1986 (Clancy and Rusch, 1989). The amplitudes of the annual and semi-annual oscillation in temperature calculated from our data are compared with the predictions of MSISE-90 (Hedin, 1991). Monthly averaged OH(3, 1) and (4, 2) band brightnesses are compared with the results of the model of Le Texier et al.(1987). A comparison of model predictions with observations provides an important test for the theoretical understanding of mesospheric transport processes, particularly the relative roles of diffusive and advective transport.

2. OBSERVATIONS AND RESULTS

Observations were made in the zenith direction at Maynooth with a Fourier transform infrared spectrometer supplied by Bomem Inc. Our instrument uses a thermoelectrically cooled InGaAs detector, which is sensitive in the wavelength region 1–1.65 μm. This wavelength range includes the rotational bands associated with the (3, 1) and (4, 2) vibrational transitions of the OH molecule. An internal HeNe laser provides accurate data sampling, and the instrument has a maximum resolution of 2 cm^{-1}. A complete interferogram is acquired in about 5 seconds with a resolution of 4 cm^{-1} which we have found to be the optimal setting when analysing the spectra for temperatures and integrated band brightness. The instrument has a field of view of $\approx 1.5°$ and typically 50 interferograms are co-added to increase the signal-to-noise ratio. The resulting interferogram is apodized using the Hanning window, and the spectra are obtained by calculating the Fourier transform of the apodized interferogram. The relative spectral response of the detector is determined by calibration with a low

brightness source whose area is sufficient to fill the field-of-view of the instrument completely. The low brightness source has been calibrated by comparing the output of an FTIR identical to the one used in this study, when it was illuminated with our source, to the output when it was illuminated with a similar source for which an NIST calibration has been obtained. We estimate that radiances calculated on the basis of this procedure are accurate to 15–20%. Difficulties associated with the absolute calibration of airglow instruments using an extended source due to multiple reflections were avoided by ensuring that the source was at a sufficient distance from the input port of the spectrometer (Torr et al., 1976). Figure 1 is a typical spectrum obtained following correction for instrument spectral response and shows both the OH(3, 1) and (4, 2) vibration-rotation bands before midnight on 6 May 1993.

The frequently poor observing conditions in Ireland, together with a site altitude of only 60 m above sea level, make it difficult to obtain long sequences of observations. Good quality spectra were recorded, however, with an integration time of 4.5 minutes on 114 clear nights during 1993. After compensation for detector sensitivity, a rotational temperature and integrated band brightness was calculated from the $P_1(2)$, $P_1(3)$ and $P_1(4)$ lines in the OH(3, 1) and (4, 2) band in each spectrum, following the method described by Sivjee and Hamwey (1987). These are some of the brightest lines in each band and are not affected to any significant extent by water vapour absorption (Lowe et al., 1991), although a recent report by Hammond and Espy (1994) indicates that improved temperature fits may be obtained by applying compensation for atmospheric transmission with the use of FASCOD2. The brightness of each line was determined by performing a non-linear least squares fit of a 20 cm^{-1} region centred on the line to a synthetic instrument function. The instrument function used was the Fourier transform of the apodization function operated on a delta function at the line centre.

Figure 2(a), which shows the variation in derived temperature during the night of 24 March 1993, is typical of the results obtained throughout the year. Figure 2(b) shows the corresponding brightness variations for the same night. Statistical errors on both rotational temperature and band brightness obviously depend on airglow brightness, which was found to vary by as much as a factor of three during a single night. At times of strong OH emission, statistical uncertainty in the calculated rotational temperatures fell to as low as ± 2 K. Typically, about 170 spectra were recorded in a single night during mid-winter

**Near Infrared spectrum recorded at Maynooth
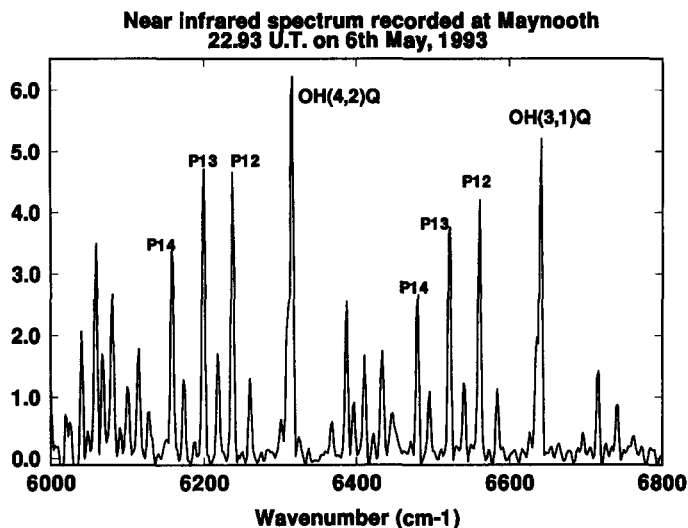22.93 U.T. on 6th May, 1993**

Fig. 1. Near infrared spectrum recorded at Maynooth on 6 May 1993 at 22.93 U.T. (integration time: 4.5 minutes). The 0-branch and the P12, P13 and P14 lines of both the OH(4, 2) and (3, 1) bands are labelled in each case.

decreasing to only about 50 in mid-summer. Figure 3(a) and (b) summarizes all the temperature results obtained in this study, and shows the well known winter-summer variation for a mid-latitude station, with the minimum in summer and maximum in winter. The generally accepted explanation of this apparent inversion is that the cold summer (warm winter) mesopause is maintained through adiabatic cooling (warming) produced by a strong summer-to-winter meridional cell which is driven by breaking vertically propagating gravity waves (Garcia and Solomon, 1985). Gaps in the data shown in Fig. 3(a) and (b) are caused by unsuitable observing conditions, and the figures indicate the fraction of time typically available for optical airglow measurements in Ireland.

3. ANNUAL AND SEMIANNUAL TEMPERATURE VARIATIONS

An average value of temperature has been calculated for each night on which data was recorded and is plotted in Fig. 4 for both the OH(3, 1) and (4, 2) bands. Also shown in this figure are the temperature results obtained by Clancy and Rusch (1989) from data recorded by the Solar Mesosphere Explorer (SME) satellite for an altitude of 86.5 km at a latitude of 50°N. The close correspondence between the SME results and the data obtained in this study confirm that the instrument performance and methods used to calculate temperatures are reliable. Temperatures calculated from the (4, 2) band are almost always

higher than those from the (3, 1) band, as illustrated in Fig. 4. One possible reason for the temperature difference might be the Einstein A coefficients for various rotational transitions used in the calculation of rotational temperature. All temperature and band brightness values reported here were calculated using the Mies (1974) transition probabilities. We also calculated temperatures for both bands using coefficients tabulated by Turnbull and Lowe (1989) and Nelson et al. (1990). Values of absolute temperature determined using all three sets of coefficients showed very good agreement, the largest variation having a value of only 2.3 K which occurred when using the Nelson et al. (1990) and Turnbull and Lowe (1989) transition probabilities for the (3, 1) band. In the case of the three sets of coefficients, temperatures derived from the OH(4, 2) band remain ~5 K above those from the (3, 1) band on average throughout the year, with the Turnbull and Lowe (1991) values giving marginally better agreement. Band brightnesses calculated using the Einstein coefficients reported by Mies (1974) and Turnbull and Lowe (1989) are also in very good agreement; the somewhat lower transition probabilities quoted by Nelson et al. (1990) result in an increase in the value of band brightness by approximately 40%, however.

Reports of higher vibrational levels showing higher rotational temperature have often been interpreted to indicate that emissions from higher vibrational levels originate from greater altitudes (Sivjee and Hamwey, 1987, and references therein). Sivjee and Hamwey

Mesopause temperature calculated from
OH(3,1) band 24th March, 1993

Time U.T.

Integrated band brightness for
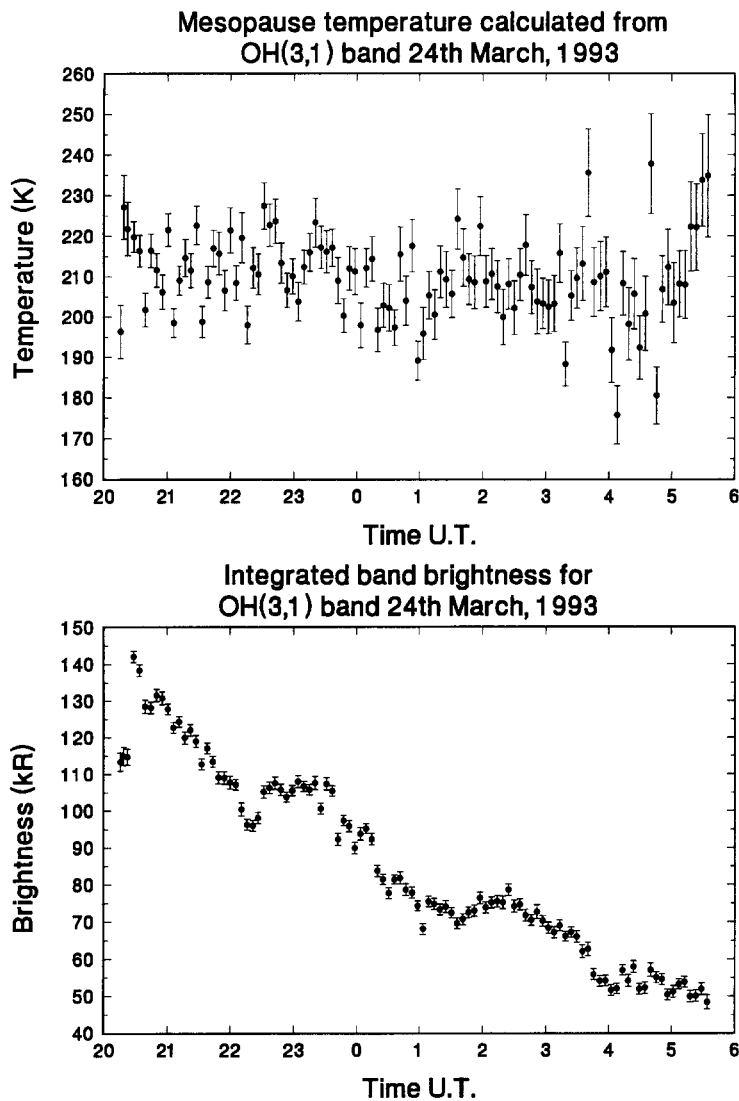## OH(3,1) band 24th March, 1993

Time U.T.

Fig. 2. (a) Mesopause temperatures calculated from OH(3, 1) band recorded at Maynooth on the night of 24/25 March 1993. (b) OH(3, 1) integrated band brightnesses calculated from spectra recorded at Maynooth on the night of 24/25 March 1993.

(1987) report that differences in T can vary from a few degrees to zero depending on location and season. Lowe et al. (1991), for example, found no significant difference in the average temperature derived from vibration bands $v' = 3-7$ during summer at high latitude. López-Moreno et al. (1987) presented results on the altitude distribution of vibrationally excited states of hydroxyl at levels $v' = 2-7$, derived from rocket photometry data. Their results show an altitude distribution which is dependent on vibrational level. The lower levels $v' = 2, 3$ have peak concentrations centred

on 85 km, while the corresponding maxima occur some 5 km higher in the upper levels. Mcdade (1991), on the other hand, predicts that the altitude difference between the lowest and highest vibrational levels should not exceed 2 km based on model calculations. Temperature gradients as large as 10 K per km in the mesopause region have been inferred by Schubert et al. (1990), from a comparison of temperatures calculated from different pairs of vibration–rotation lines in the OH(6, 2) band. On the basis of such a steep gradient, a temperature difference of 6 K between the
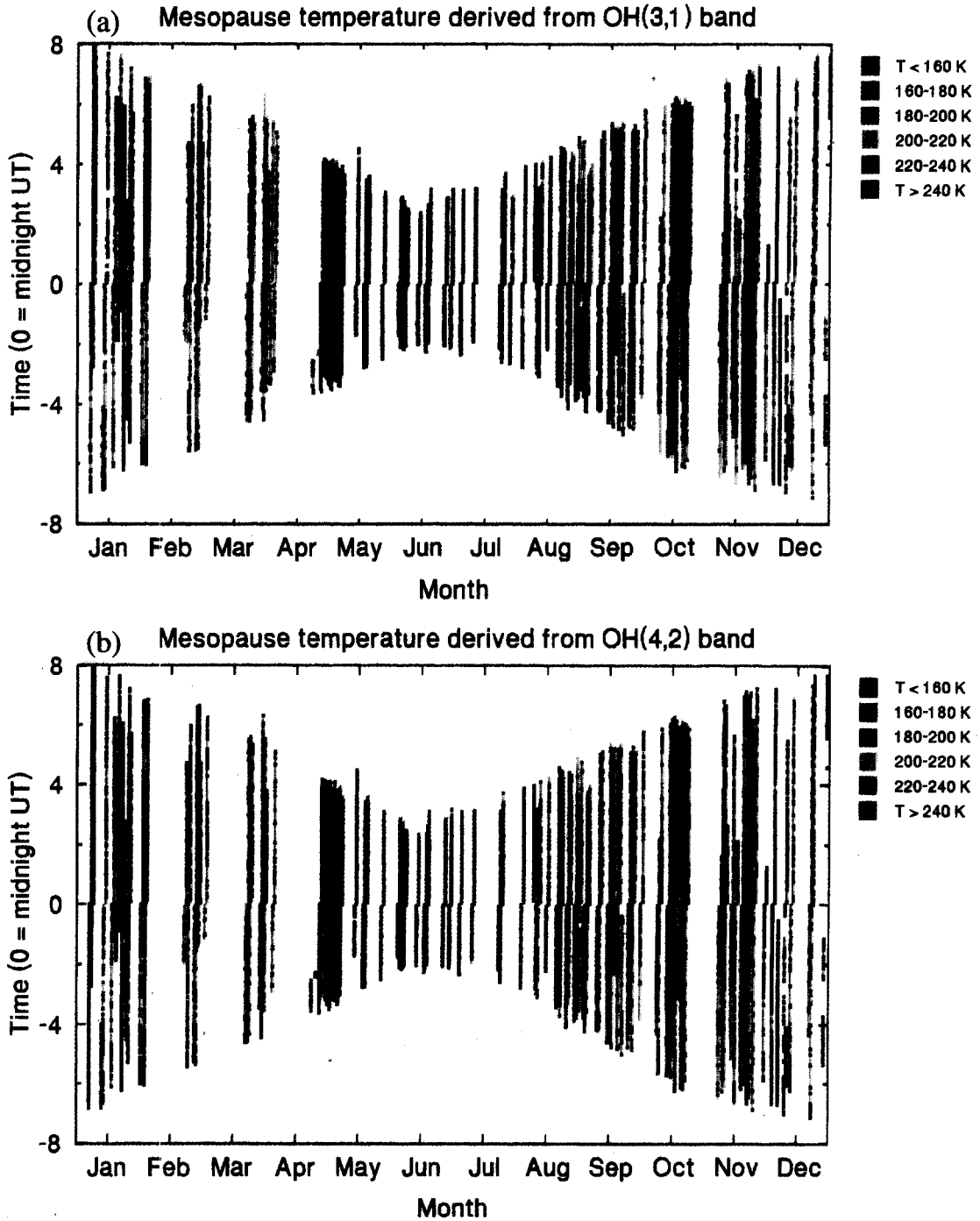
Fig. 3. Summary of all mesopause temperatures derived from OH(3, 1) band recorded at Maynooth, during 1993. (b) Summary of all mesopause temperatures derived from OH(4, 2) band recorded at Maynooth, during 1993.
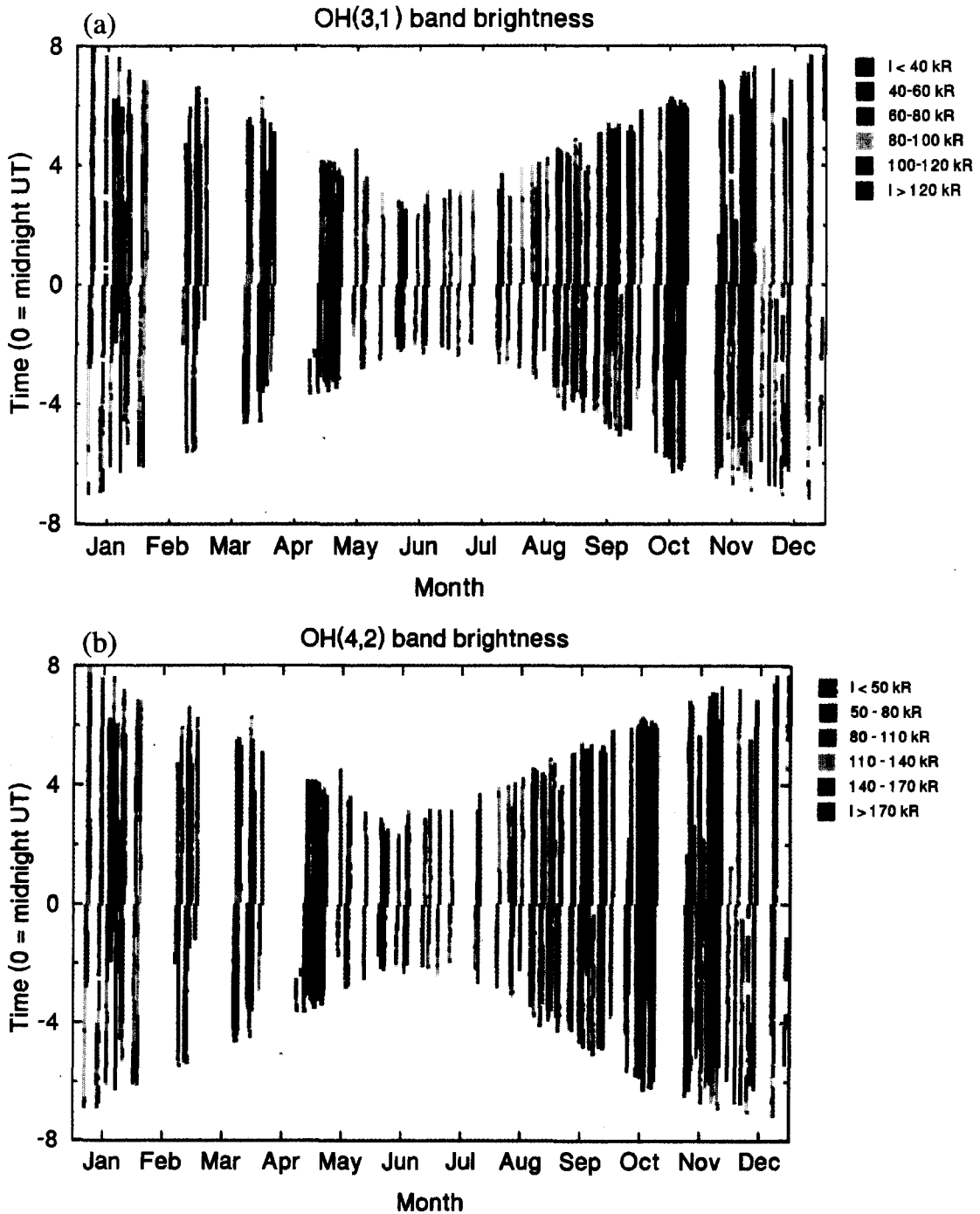
Fig. 5. (a) Summary of all OH(3, 1) band brightnesses measured at Maynooth, during 1993. (b) Summary of all OH (4, 2) band brightnesses measured at Maynooth, during 1993.
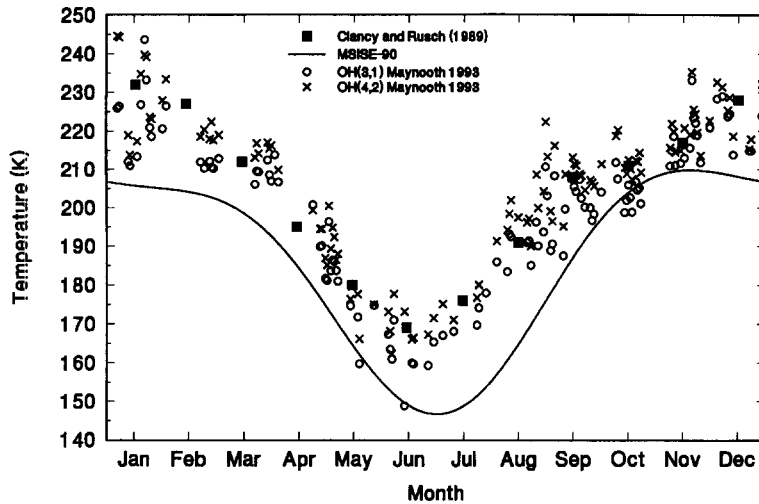
Fig. 4. Annual variation in measured [OH(3, 1) (open circles) and OH(4, 2) (x)] and modelled [MSISE-90(solid line)] mesopause temperatures at Maynooth. Temperature values obtained by Clancy and Rusch (1989) (solid squares) for an altitude of 86.5 km at a latitude of 50° N are included for comparison.

(3, 1) and (4, 2) band could be generated by an altitude difference of only 0.5 km.

Figure 4 also shows the predictions of the MSISE-90 model (Hedin, 1991) for an altitude of 87 km at Maynooth. The model appears consistently to under-estimate the mean temperature, by about 15–20 K. Harmonic analysis, similar to that reported recently by Reddi *et al.* (1993) for a low latitude station, has been applied to the nightly averaged values of tem-perature to uncover the underlying annual and semi-annual oscillations. Table 1 shows the amplitudes and phases of these two components for both the OH(3, 1) and (4, 2) bands, together with the annual mean temperature. The two data sets show remarkable agreement in both the annual and semiannual com-ponent, even though the annual mean value of tem-perature for the two bands differs by 6 K. Agreement between the MSISE-90 model and our results is excel-lent in the case of the amplitude of the annual and semiannual component; however, the model appears to overestimate the phase of the semiannual com-

ponent by about 40–50%. This degree of cor-respondence between the model and our results is a very encouraging result for the extension of the MSIS model to lower altitudes for a mid-latitude station, the only reservation being the offset in the absolute value of temperature predicted.

4. DIURNAL AND SEASONAL BRIGHTNESS VARIATIONS

Figure 5(a) and (b) summarizes the brightness measurements of the OH(3, 1) and (4, 2) bands obtained in this study, respectively. In interpreting these results, the following cautionary remarks apply. The data presented here have not been corrected for atmospheric extinction and it is likely that this con-tributes a much larger degree of uncertainty to the measurements than the statistical errors plotted in Fig. 2(b). While observations were made only when sky conditions were clear as determined by eye, local

Table 1. Observed [OH(3, 1) and (4, 2) results for 1993] and predicted (MSISE-90) mean, annual and semiannual variations in mesopause temperature at Maynooth

	Annual mean temperature/K	Annual component		Semiannual component	
		Amplitude/K	Phase/days	Amplitude/K	Phase/days
OH(3, 1)	200 ± 19	27 ± 1	95 ± 2	7 ± 1 K	−51 ± 9
OH(4, 2)	206 ± 19	27 ± 1	95 ± 2	8 ± 1 K	−43 ± 1
MSISE-90	185 ± 22	30.1 ± 0.2	95.3 ± 0.6	9 ± 0.2 K	−99 ± 1

weather conditions can be very variable even over periods as short as 1 hour.

All times and seasons are equally variable, however, so that we do not anticipate the introduction of diurnal or seasonal effects as a result of variable atmospheric conditions.

Bearing in mind these reservations there are, nevertheless, some interesting patterns which are immediately evident in Fig. 5(a) and (b). Both figures show the large degree of variability in OH brightness and are very similar in appearance apart from the fact that the brightness of the (4, 2) band is typically about 30% greater than that of the (3, 1) band. The annual mean brightness of the OH(3, 1) band was found to be 75 ± 18 kR, while that of the (4, 2) band was 106 ± 26 Kr. Figure 5(a) and (b) shows what appears to be a sustained maximum in the April/May period, and a rather obvious minimum in October, particularly after midnight.

Diurnal variations of OH emission brightness have been studied by many observers, e.g. Wiens and Weill (1973); Takahashi *et al.* (1977); Abreu and Yee (1989), most of whom have found that the variation is a function of both latitude and season. Figure 6 shows the nocturnal variation in OH(3, 1) brightness found in this study for each month of the year, and is in good agreement with earlier reports. Generally, the brightness is highest early in the night and decreases towards dawn as illustrated in Fig. 2(b). Data shown in Fig. 6 for July appear to deviate from this pattern with an increase in brightness following midnight. Figure 7, for example, shows the brightness of the OH(3, 1) emission recorded at Maynooth on 5 July 1993. Similar behaviour was found by Abreu and Yee (1989) and Wiens and Well (1973) in summer solstice data at low latitudes. A steady decrease in OH brightness from sunset to sunrise is predicted by photochemical models, based on decreasing concentrations of odd hydrogen and odd oxygen, as a result of the absence of photolysis of O_2 and H_2O (Abreu and Yee, 1989). An increase in brightness, such as that observed in the July data recorded here, cannot be explained by photochemical models, however. Density and temperature perturbations (Takahashi *et al.*, 1977), and variations in eddy diffusion (Moreels *et al.*, 1977), resulting from tidal wave energy input, have been advanced as possible explanations of the increase in OH brightness following midnight, but as yet a completely satisfactory explanation remains to be found. Garcia and Solomon (1985) cite the poor understanding of diurnal variations in OH emissions as the reason for omitting them from their study of the dynamics and chemistry of the mesosphere and lower thermosphere, preferring instead the relatively better

understood airglow features of atomic oxygen and ozone. More recently, Rodrigo *et al.* (1991) have compared the diurnal evolution of the Meinel OH emissions for midlatitude equinox conditions, predicted by a non-steady one-dimensional model atmosphere, with both ground based (Krassovsky *et al.*, 1962) and rocket measurements (López-Moreno et al, 1987) of these emissions. The agreement found between the measured and predicted values was interpreted as a validation of the model. Figure 8 shows the diurnal variation of the number of particles of OH in a centimetre squared column for vibrational levels $v' = 3$ and $v' = 4$, taken from Rodrigo *et al.* (1991). The same parameters derived from the hourly averaged OH brightness values obtained in this study for the months of March and September are also included in Fig. 8. The general trend observed in the data is well reproduced by the model, although the absolute values tend to be somewhat higher, and the gradient of the night time decrease somewhat larger in the measurements. Our observations agree very well with the results from Krassovsky *et al.* (1962) and López-Moreno *et al.* (1987). The measurements of twilight to dawn variations in OH brightness obtained here used in conjunction with the model of Rodrigo *et al.* (1991) would enable estimates of the variation in atomic oxygen and atomic hydrogen at mesopause altitudes to be obtained. Obviously, such estimates would be vulnerable to the uncertainties of both the model and the measurements.

There are very few reports of OH brightness measurements, particularly for low vibrational levels, which might be used to validate predictions of seasonal variations in OH emission by dynamical and photochemical models (Le Texier *et al.*, 1987). The highly variable nature of OH emission brightness (as much as a factor of four in a single night, Scheer and Reisin, 1990) makes the detection of seasonal variations, predicted to be of the order of 10–20% at mid-latitudes (Le Texier *et al.*, 1987), very difficult. The steady decrease in OH brightness during the night observed in most of the data reported here meant that any search for a seasonal variation had to be confined to an equal time interval throughout the year. At our latitude, the short summer nights prevent us from obtaining sequences of data longer than about 4 hour centred on midnight. Monthly averaged brightnesses were calculated for periods of 2, 3 and 4 hour centred on midnight for all of the 1993 data. All three results showed behaviour similar to that shown in Fig. 9(a), which depicts the monthly averaged brightness of the OH(3, 1) band for 4 hour centred on midnight. Figure 9(b) shows the corresponding variation for the (4, 2) band. Both bands show similar behaviour with a
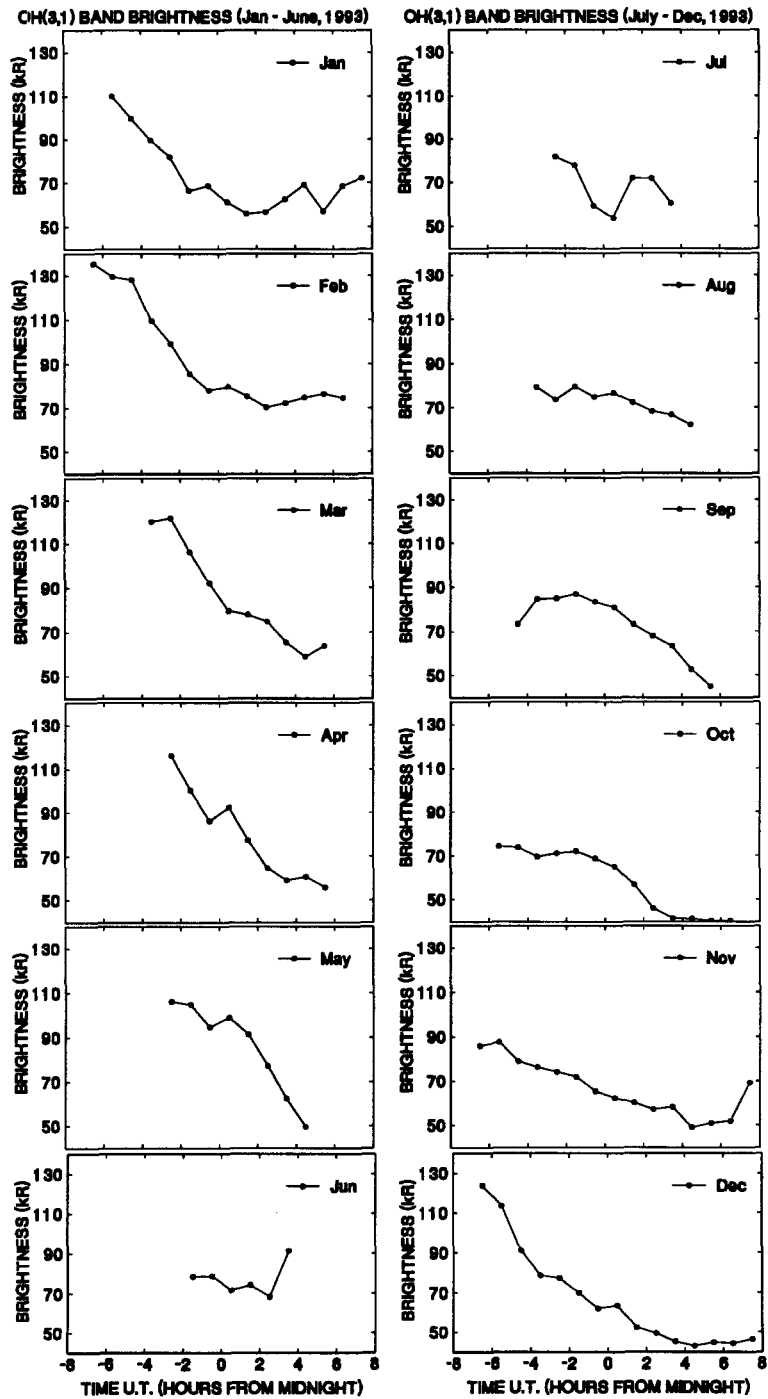
Fig. 6. Nocturnal variation in OH(3, 1) band brightness as a function of month at Maynooth, during 1993.

Integrated band brightness for OH(3,1) band 5th July, 1993
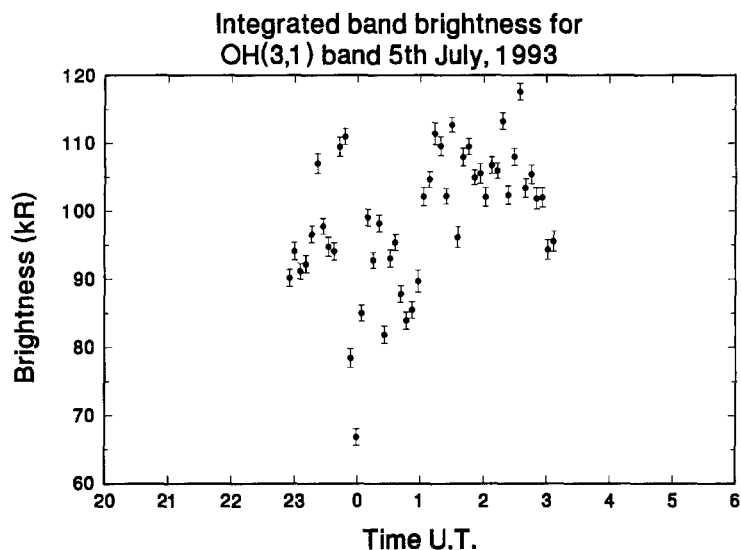

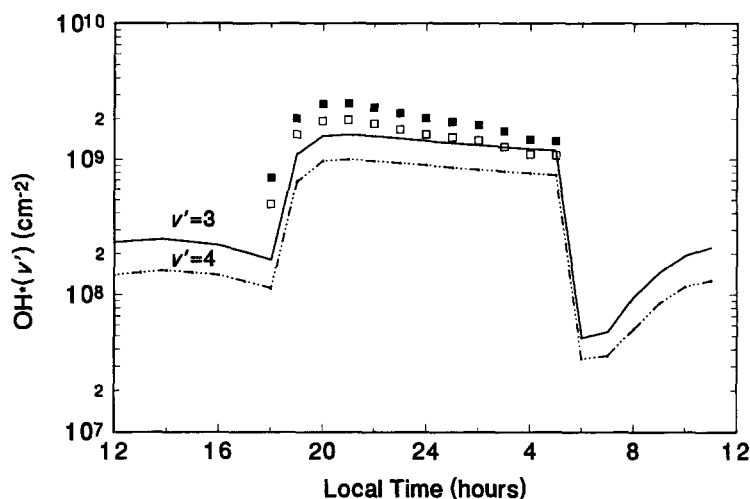Fig. 7. OH(3, 1) integrated band brightnesses from spectra recorded on 5 July 1993.

Fig. 8. Diurnal variation of the number of OH particles in a centimetre squared column for vibrational levels $v'=3$ and $v'=4$. Solid and dashed lines are from Rodrigo *et al.* (1991); solid squares ($v'=3$) and open squares ($v'=4$) are derived from the hourly averaged OH emission brightnesses recorded at Maynooth, in March and September 1993.

broad minimum in winter and maxima in May and September. These maxima are separated by a local minimum in July, which is quite pronounced in the (3, 1) band. The increase in brightness following the winter minimum is interrupted in both bands during April, and in the case of the (4, 2) band the brightness even shows a decrease during April. Both bands show reasonable agreement in brightness between December and January, indicating the stability and

consistency of the instrument brightness calibration throughout the year.

Figure 9(a) and (b) also shows the predictions of the model of Le Texier *et al.* (1987) for both low (5, 3) and high (9, 3) vibrational levels at 54°N. The model deals separately with low and high vibrational levels on account of the possibility of populating vibrational levels, $v' < 6$, by the per hydroxyl-oxygen (PHO) reaction:
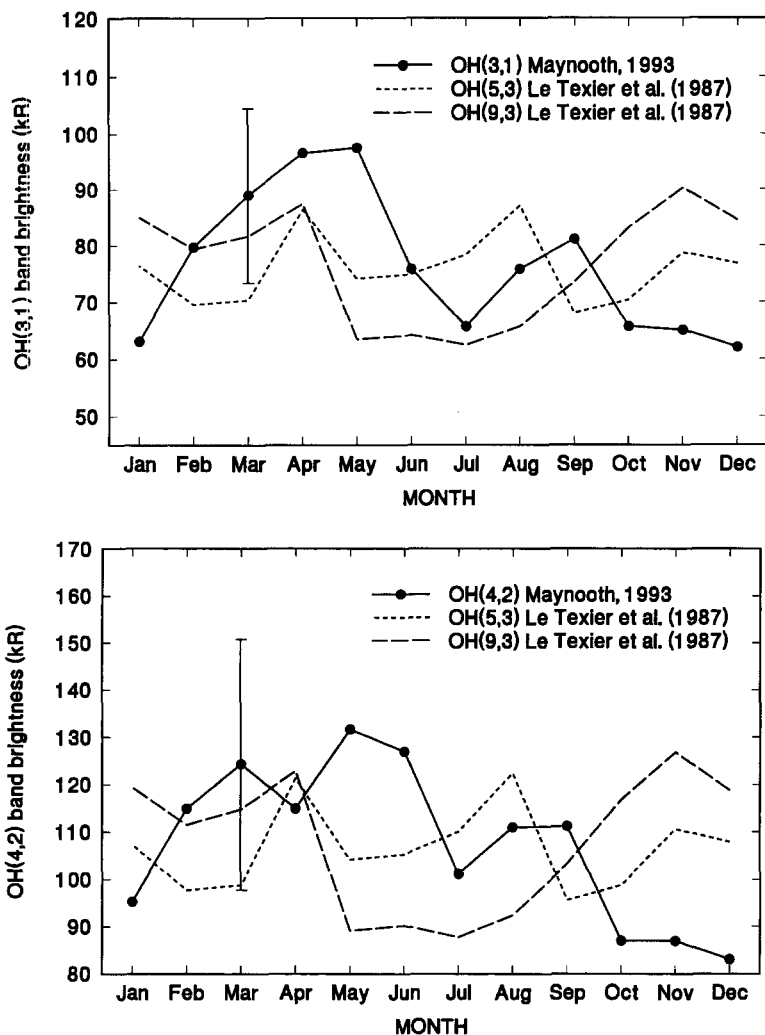
Fig. 9. (a) Annual variation in OH integrated band brightness at Maynooth during 1993. The solid circles represent the OH(3, 1) measured data for 4 hour centred on midnight. The error bar represents the standard deviation on all brightness measurements obtained within the 4 hour centred on midnight for the month of March, and is typical of the data. The dashed lines are the predictions of the model of Le Texier *et al.* (1987) for emissions from both low [OH(5, 3)] and high [OH(9, 3)] vibrational levels. The model was normalised to the Maynooth data by assigning the undeviated brightness to the annual mean of the measured values. Deviations from this value were calculated by assuming that a change in brightness equal to the annual mean represented a 100% deviation. (b) As in Fig. 9(a), but in this case the solid circles represent the OH(4, 2) measurements.

$$HO_2 + O \rightarrow OH^* + O_2.$$
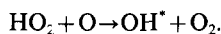
If this reaction was not an effective source of vibrationally excited OH, the seasonal behaviour relative to the annual mean would be similar for all vibrational levels (Le Texier *et al.*, 1987). Recent reports, however, suggest that this reaction may not be a source of vibrationally excited OH (Mcdade and Llewellyn, 1987; Kaye, 1988); consequently we com-

pare our results with the predictions of the model for both low and high vibrational levels.

The model predictions for vibrational levels $v' > 6$ are predominant of an annual variation with a minimum in summer. This is a result of the fact that the OH nightglow emission seasonal variation is dominated by the atomic oxygen mixing ratio variation, with its amplitude attenuated by temperature effects. The introduction of the PHO reaction to the model,
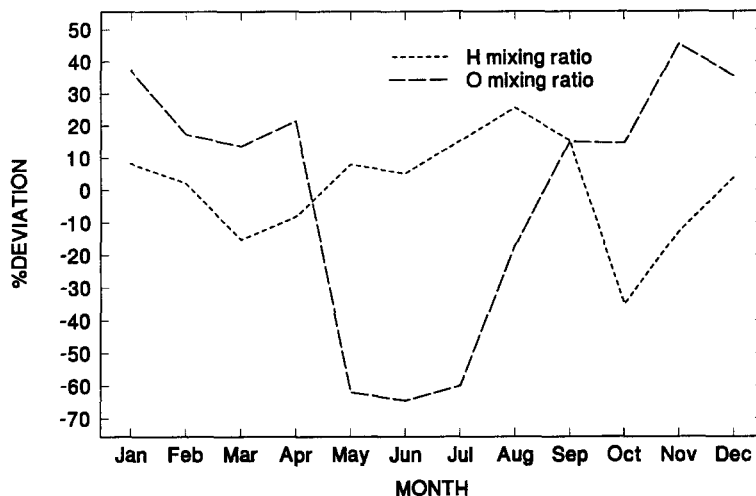
Fig. 10. Annual variation in atomic hydrogen (short dash) and atomic oxygen (long dash) mixing ratio at the mesopause for a latitude of 54°N [from Le Texier *et al.*(1987)].

populating excited OH vibrational levels, $v' < 6$, results in the seasonal behaviour of OH emission brightness being controlled by both the atomic oxygen and atomic hydrogen mixing ratios, μ_O and μ_H respectively. Figure 10 shows the annual variation in the atomic oxygen and atomic hydrogen mixing ratios, for a station at 54°N latitude, taken from Le Texier *et al.* (1987). The interaction of these terms is quite complex, the atomic hydrogen ratio depending on the rate of advection of water vapour from the stratosphere to the mesosphere, and the efficiency of photolysis of water vapour in the mesosphere which is a function of latitude and season. The atomic oxygen behaviour is controlled by localized phenomena restricted to latitudes between 45° and 75° and altitudes between 80 and 95 km. In this region, vertical advection attains its maximum value in the mesosphere. This very fast upward motion locally dominates the transport of odd-oxygen, bringing odd-oxygen poor air to the mesopause, and leads to a very deep summer minimum in the oxygen density at 85–90 km. This same rapid upward motion is responsible for an increase in water vapour at the mesopause, thus the two terms oppose one another resulting in the prediction of a largely semiannual behaviour, with maxima in April and August, and amplitude variations in the range 10–20%.

While neither of the model predictions show obvious agreement with the data obtained in this study, those based on the inclusion of the PHO reaction are favoured. Maximum disagreement between the models and the data is observed during the winter period, with the model omitting the PHO reaction as the worst offender as shown in Fig. 9(a) and (b). The broad winter minimum observed in our data for both bands, but not predicted by either version of the model, might suggest that insolation-driven photochemistry, plays a larger part in the control of OH emission brightness for low vibrational levels at 54°N than proposed in the model. A local minimum is observed in the summer period as predicted by the model including the PHO reaction, particularly the two maxima near the equinoxes, although the peaks occur a month later in the data and are asymmetrical. The amplitude of the variations predicted is somewhat lower that the 20–30% observed in the data. One interesting feature in Fig. 10 is the minimum in the atomic hydrogen mixing ratio in October, which coincides with the October brightness minimum shown in Fig. 5(a) and (b) for the early morning hours.

Shepherd *et al.* (1993) have recently reported large amplitude longitudinal structure in atomic oxygen 557.7 nm and OH(8, 3) airglow emission rates observed with the WINDII instrument onboard the Upper Atmosphere Research Satellite. It is believed that these data represent a superposition of planetary wave structures with zonal wave numbers 1 and 2. The magnitude of the longitudinal airglow variations together with the absence of such large fluctuations in ground-based brightness data, lead Shepherd *et al.* to conclude that these fluctuations are not the result of solar-driven photochemistry, but must instead originate at the Earth or in the lower atmosphere. The

results reported by Shepherd *et al.* are preliminary, however, and require the emission rate data from the WINDII instrument to be used in conjunction with ground-based measurements, before the presence of the apparent planetary waves can be confirmed.

6. SUMMARY

Measurements of mesopause temperature and OH(3, 1) and (4, 2) integrated band brightness obtained from airglow emissions recorded at Maynooth during 1993 have been presented. The temperature data are in very good agreement with the results obtained from the SME satellite. A comparison of the data recorded here with predictions of the MSISE-90 model shows the model to underestimate the temperature by 15–20 K. Nevertheless, the model accurately predicts the amplitude of the annual and semiannual components remarkably well. It also predicts the correct phase of the annual component, but appears to overestimate the phase of the semiannual oscillation. We believe that differences in the value of temperature obtained from the two OH bands result from the (4, 2) emission originating at a somewhat higher altitude than the (3, 1) band. No obvious diurnal variation in temperature was found in the data.

Diurnal variations in OH brightness for both (4, 2)

and (3, 1) bands generally showed a steady decrease from sunset to sunrise in agreement with photochemical models. This pattern appeared to change near summer solstice, however, with a post-midnight increase in brightness occurring. Our data showed some elements of correspondence with the predictions of the model of Le Texier *et al.* (1987) particularly a pair of maxima near the equinoxes. The model does not predict the broad winter minimum observed in both bands, and it is possible that seasonal behaviour is influenced more by photochemistry than anticipated by the model. Our study will continue over the next few years, and it will be interesting to see if the patterns observed here persist in the data. It seems likely that present models of OH emission brightness will require further refinement so that they accurately describe the complex behaviour resulting from the combined seasonal and diurnal variation.

REFERENCES

Abreu V. J. and Yee J. H. — 1989 — Diurnal and seasonal variation of the night-time OH (8-3) emission at low latitudes. *J. geophys. Res.* **94**, 11,949–11,957.

Baker D. J. and Stair Jr, A. T. — 1988 — Rocket measurements of the altitude distributions of the hydroxyl airglow. *Physica Scripta* **37**, 611–622.

Clancy R. T. and Rusch D. W. — 1989 — Climatology and trends of mesospheric (58–90 km) temperatures based upon 1982–1986 SME limb scattering profiles. *J. geophys. Res.* **94**, 3377–3393.

Garcia R. R. and Solomon S. — 1985 — The effect of breaking gravity waves on the dynamics and chemical composition of the mesosphere and lower thermosphere. *J. geophys. Res.* **90**, 3850–3868.

Hammond M. R. and Espy P. J. — 1994 — Optical OH transitions in the near infrared for rotational temperature determination. In preparation for *J. geophys. Res.*

Hecht J. H., Walterscheid R. L., Sivjee G. G., Christensen A. B. and Pranke J.B. — 1987 — Observations of wave-driven fluctuations of OH nightglow emission from Sondre Stromfjord, Greenland. *J. geophys. Res.* **92**, 6091–6099.

Hedin A. E. — 1991 — Extension of the MSIS thermospheric model into the middle and lower atmosphere. *J. geophys. Res.* **96**, 1159–1172.

Hernandez G., Smith R. W. and Conner J. F. — 1992 — Neutral wind and temperature in the upper mesosphere above south pole, Antarctica. *Geophys. Res. Lett.* **19**, 53–56.

Kaye J. A. — 1988 — On the possible role of the reaction $O \rightarrow HO_2 + OH + O_2$ in OH airglow. *J. geophys. Res.* **93**, 285–288.

Krassovsky V. I. 1972 Infrasonic variations of OH emission in the upper atmosphere. *Ann. Geophys.* **28**, 739–746.

Krassovsky V. I., Shefov N. N. and Yarin V. I. 1962 Atlas of the airglow spectrum 3000–12400 Å. *Planet. Space Sci.* **9**, 883–915.

Le Texier H., Solomon S. and Garcia R. R. 1987 Seasonal variability of the OH Meinel bands. *Planet. Space Sci.* **35**, 977–989.

López-Moreno J. J., Rodrigo R., Moreno F., López-Puertas M. and Molina A. 1987 Altitude distribution of vibrationally excited states of atmospheric hydroxyl at levels $v = 2$ to $v = 7$. *Planet. Space Sci.* **35**, 1029–1038.

Lowe R. P., Gilbert K. L. and Turnbull D. N. 1991 High latitude summer observations of the hydroxyl airglow. *Planet. Space Sci.* **39**, 1263–1270.

Mcdade I.C. and Llewellyn E. J. 1987 Kinetic parameters related to sources and sinks of vibrationally excited OH in the nightglow. *J. geophys. Res.* **92**, 7643–7650.

Mcdade I. C. 1991 The altitude dependence of the OH $(X^2\Pi)$ vibrational distribution in the nightglow: some model expectations, *Planet. Space Sci.* **39**, 1049–1057.

Meinel A. B. 1950a OH emission bands in the spectrum of the night sky. *Astrophys. J.* **111**, 555–564.

Meinel A. B. 1950b OH emission bands in the spectrum of the night sky. *Astrophys. J.* **112**, 120–130.

Mies F. H. 1974 Calculated vibrational probabilities of OH $(X^2\Pi)$ *J. Molec. Spectros.* **53**, 150–188.

Moreels G., Megie G., Vallance Jones A. and Gattinger R. L. 1977 An oxygen-hydrogen atmospheric model and its application to the OH emission problem. *J. atmos. terr. Phys.* **39**, 551.

Myrabo H. K., Deehr C. S. and Viereck R. 1987 Polar mesopause gravity wave activity in the sodium and hydroxyl night airglow. *J. geophys. Res.* **92**, 2527–2534.

Nelson Jr D. D., Schiffman A. and Nesbitt D.J. 1990 H + O_3 Fourier-transform infrared emission and laser absorption studies of OH$(X^2\Pi)$ radical: an experimental dipole moment function and state-to-state Einstein A coefficients. *J. chem. Phys.* **193**, 7003–7019.

Reddi C. R., Rajeev K. and Rakumar G. 1993 Annual and semiannual oscillations at the mesopause levels over Trivandrum (8.5°N, 78°E). *J. geophys. Res.* **98**, 8925–8931.

Rodrigo R., López-Gonzalez M. J. and López-Moreno J. J. 1991 Variability of the neutral mesospheric and lower thermospheric composition in the diurnal cycle. *Planet. Space Sci.* **39**, 803–820.

Shepherd G. G., Thuillier G., Solheim B. H., Chandra S. Cogger L. L. 1993 Longitudinal structure in atomic oxygen concentrations and observed with WINDII on OARS. *Geophys. Res. Lett.* **20**, 1303–1306.

Scheer J. and Resin E. R. 1990 Rotational temperatures for OH and O_2 airglow bands measured simultaneously from El Leoncito (31°48'S). *J. atmos. terr. Phys.* **52**, 47–57.

Schubert G., Walterscheid R. L. and Hecht J. H. 1990 Temperature gradients at mesopause heights inferred from OH nightglow data. *J. geophys. Res.* **95**, 19,061–19,067.

Sivjee G. G. 1992 Airglow hydroxyl emissions. *Planet. Space Sci.* **40**, 235–242.

Sivjee G. G., Walterscheid R. L., Hecht J. H., Hamwey R. M., Schubert G. and Christensen A. B. 1987 Effects of atmospheric disturbances on polar mesopause airglow OH emissions. *J. geophys. Res.* **92**, 7651–7656.

Sivjee G. G. and Hamwey R. M. 1987 Temperature and chemistry of the polar mesopause OH. *J. geophys. Res.* **92**, 4663–4672.

Takahashi H., Sahai Y., Clemesha B. R., Batista P. P. and Teixeira N. R. 1977 Diurnal and seasonal variations of the OH (8, 3) airglow band and its correlation with OH 5577 Å. *Planet. Space Sci.* **25**, 541–547.

Torr M. R., Hays P. B., Kennedy B. C. and Torr D.G. 1976 Photometer calibration error using extended standard sources. *Appl. Opt.* **15**, 600–602.

Turnbull D. N. and Lowe R. P. 1989 New hydroxyl transition probabilities and their importance in airglow studies. *Planet. Space Sci.* **37**, 723–738.

Turnbull D. N. and Lowe R. P. 1991 Temporal variations in the hydroxyl nightglow observed during ALOHA-90. *Geophys. Res. Lett.* **18**, 1345–1348.

Viereck R. A. and Deehr C. S.   1989   On the interaction between gravity-waves and the OH Meinel (6-2) and the O_2 atmospheric (0, 1) bands in the polar night airglow. *J. geophys. Res.* **94,** 5397–5404.

Wiens R. H. and Weill G.   1973   Diurnal, annual and solar cycle variations of hydroxyl and sodium nightglow intensities in the Europe-Africa sector. *Planet. Space Sci.* **21,** 1011–1027.